The Effect of Podoplanin Inhibition on Lymphangiogenesis Under Pathological Conditions

Yuko Maruyama,[1] Kazuichi Maruyama,[2] Yukinari Kato,[3] Kentaro Kajiya,[4] Satoru Moritoh,[2] Kotaro Yamamoto,[2] Yuko Matsumoto,[4] Mika Sawane,[4] Dontscho Kerjaschki,[5] Toru Nakazawa,[2] and Shigeru Kinoshita[1]

[1]Department of Ophthalmology, Kyoto Prefectural University of Medicine, Kyoto, Japan
[2]Tohoku University Graduate School of Medicine, Department of Ophthalmology, Sendai, Japan
[3]Department of Regional Innovation, Tohoku University Graduate School of Medicine, Sendai, Japan
[4]Shiseido Innovative Science Research Center, Yokohama, Japan
[5]Department of Pathology, Medical University Vienna, Vienna, Austria

Correspondence: Kazuichi Maruyama, Tohoku University Graduate School of Medicine, Department of Ophthalmology and Visual Science, 1-1 Seiryo-cho Aoba-ku, Sendai, Japan;
maruyama-k@oph.med.tohoku.ac.jp

Submitted: December 5, 2013
Accepted: May 25, 2014

Citation: Maruyama Y, Maruyama K, Kato Y, et al. The effect of podoplanin inhibition on lymphangiogenesis under pathological conditions. *Invest Ophthalmol Vis Sci*. 2014;55:4813–4822. DOI:10.1167/iovs.13-13711

Purpose. Podoplanin has been shown to be a reliable marker of lymphatic endothelium, but its role in the lymphatic system has not been well investigated. The purpose of this study is to investigate the role of podoplanin in lymphangiogenesis and macrophage functions under inflammatory conditions.

Methods. Mouse corneal suture and ear section models were used to induce lymphangiogenesis and macrophage infiltration. Antilymphatic vessel endothelial hyaluronan-1 (Anti-LYVE-1) antibody was used to visualize lymphatic vessels. Thioglycollate-induced macrophages (mps) were collected and cultured with lipopolysaccharide (LPS), IFN-γ, and anti-mouse podoplanin antibody (PMab-1). Podoplanin, NF-κB, and mitogen-activated protein kinase (MAPK) pathway expression were detected by Western blot analysis. The TNF-α secretion was measured by ELISA.

Results. Administration of PMab-1, reduced lymphangiogenesis in the corneal suture and ear wound healing models. Also, PMab-1 suppressed mps infiltration at the site of wound healing. Moreover, administration of PMab-1 led to a significant suppression of the rejection reaction in the corneal transplantation model. Our in vitro experiments showed that PMab-1 suppressed TNF-α secretion from mps under inflamed conditions, especially secretion caused by LPS stimulation. We confirmed the effect of PMab-1 on mps under inflamed conditions with a Western blot experiment, which clearly showed that the phosphorylation signal of the MAPK and NF-κB pathways was suppressed by PMab-1.

Conclusions. Podoplanin neutralization resulted in inhibition of lymphatic growth associated with corneal and ear wound healing as well as mps inflammation. These data suggest that podoplanin is a novel therapeutic target for suppressing lymphangiogenesis and inflammation.

Keywords: lymphangiogenesis, macrophage, podoplanin

Podoplanin (Aggrus) is a mucin-like sialoglycoprotein that is highly expressed in lymphatic endothelial cells (LECs), kidney podocytes, and type-I alveolar cells. Podoplanin is expressed in LECs and not in vascular endothelial cells.[1] Therefore, it is used as a marker for LECs.

Podoplanin has been reported in many tumors, such as different types of squamous cell carcinoma, Kaposi's sarcoma, and brain tumors.[2–6] Recent studies have suggested that podoplanin overexpression is associated with tumor metastasis and poor prognosis.[2,3,5–11] Anti-podoplanin antibodies have been shown to delay podoplanin-induced platelet aggregation via podoplanin/C-type lectin receptor–2 (CLEC-2) interaction, and to inhibit significantly the number of metastatic lung nodules in studies using experimental models of metastasis in mice, suggesting that podoplanin may be a promising target for anti-metastatic drugs.[8,12–15]

It also has been reported that podoplanin is necessary for lymph/blood vessel separation at the embryonic stage.[16,17] Lymphatic vessel development begins at the cardinal vein in the embryo when venous endothelial cells give rise to form the lymph sacs. Podoplanin-deficient mice have blood/lymphatic misconnections and exhibit mortality at the embryonic/neonatal stages associated with disorganized and blood-filled lymphatic vessels, and severe edema due to abnormal blood/lymphatic vessel separation.[18]

Many previous studies report on podoplanin in tumor conditions as mentioned above. However, only a few studies have associated podoplanin with inflammatory responses using myeloid cells.[19,20] We have shown previously that CD11b-positive macrophages (mps) were critical for the development of inflammation-dependent lymphangiogenesis in the cornea.[21] We also have shown that the lymphatic vessel maintenance in the cornea is dependent on the presence of mps.[22] We expected that podoplanin might be related to mps inflammation and lymphangiogenesis. In the corneal suture placement model, some cytokines, such as VEGF-A and IL-1β secreted from

mps have critical roles inducing lymphatic vessels.[23,24] It has been shown that podoplanin is expressed on inflammatory mps and is upregulated in response to some inflammatory cytokines in mice.[20] However, the details of the relationship between podoplanin function in mps and lymphangiogenesis still are unclear.

In this study, we used the podoplanin-neutralizing antibody (PMab-1) to investigate the role of podoplanin in lymphangiogenesis and macrophage (mp)-related inflammation in both in vitro and in vivo experiments.

Materials and Methods

Animals

Male BALB/c mice (Japan CREA, Shizuoka, Japan) 8 to 10 weeks old were used in the corneal transplantation and ear section models. Male C57BL/6 mice (Japan CREA) 8 to 10 weeks old also were used in the corneal transplantation as well as the suture placement models and the peritoneal exudate cell (PEC) collection. All animals were treated in accordance with the Association for Research in Vision and Ophthalmology (ARVO) Statement for the Use of Animals in Ophthalmic and Vision Research, and all protocols were approved by the Committee for Animal Research of the Kyoto Prefectural University of Medicine.

Mouse Corneal Transplantation and Corneal Suture Placement

For the corneal inflammation, stromal incisions that encompassed more than 120° of the corneal circumference were made (male C57BL/6 mice, 8 to 10 weeks old) and three 11-0 nylon sutures were placed intrastromally ($n = 5$, each group). To obtain a standardized angiogenic response, the outer edge of the suture was placed halfway between the limbus and the line outlined by the 2-mm trephine. Mice were injected via tail vein with PMab-1[25] (100 μg) or PBS once per day on days 0, 1, 2, 3, and 5. The sutures were left in place for 7 days.

For the corneal transplantation experiment, male C57BL/6 mice (8 to 10 weeks old) were used as donors, and male BALB/c mice (8 to 10 weeks old) were used as hosts. Before penetrating keratoplasty (PKP) or corneal suture placement, each animal was deeply anesthetized with an intraperitoneal (IP) injection of 3 mg ketamine and 0.01 mg xylazine before the central 2-mm portion of the donor cornea was excised with Vannas scissors and secured in recipient graft beds with 8 interrupted 11-0 nylon sutures. The PMab-1 (150 μg) was injected into the subconjunctival space of each host mouse ($n = 5$, each group) at 0, 3, 5, and 7 days after corneal transplantation. The status of the corneal transplant was assessed through postoperative day 56.

Whole-Mount Corneal Staining and Morphologic Determination of Lymphangiogenesis and mp Infiltration

The mice were euthanized 7 days after transplantation or suture placement. The corneas were excised, rinsed 3 times in PBS, and fixed in 4% paraformaldehyde (PFA) overnight. They then were rinsed 3 times in PBS, blocked with 3% skim milk, and incubated overnight at 4°C with rabbit anti-mouse lymphatic vessel endothelial hyaluronan receptor–1 (LYVE-1) antibody (1:200; Reliatech, Braunschweig, Germany) and rat anti-mouse F4/80 (1:200; AbD Serotec, Oxford, UK). The tissues then were washed and stained with FITC and Cy3-conjugated secondary antibody (1:2000; Jackson ImmunoResearch Laboratories, West Grove, PA, USA). Whole-mount sections were analyzed under a fluorescence microscope (Olympus, Tokyo, Japan) and a confocal microscope (LSM 710; Carl Zeiss Meditec, Jena, Germany). Digital pictures of the flat mounts were taken with an image analysis system (Spot, Chantilly, VA, USA), and the area covered by lymphatic vessels positive for LYVE-1 was measured using ImageJ software (developed by Wayne Rasband, National Institutes of Health, Bethesda, MD, USA; available in the public domain at http://rsb.info.nih.gov/ij/index.html). The total corneal area covered by LYVE-1$^+$ vessels was outlined using the innermost vessel of the limbal arcade as the border. The area of lymphatic neovascularization within the cornea was calculated and normalized to the total corneal area (expressed as a percentage of the cornea covered by vessels). Moreover, to quantify the number of mps infiltrating the cornea, the density of F4/80 expression in matching squares 1 mm from the limbus was measured with Image J software.

Immunofluorescence Staining for F4/80, LYVE-1, Podoplanin and 4′6-Diamidino-2-Phenylindole (DAPI)

After fixation with 4% PFA at 4°C overnight, the corneal and skin samples were washed three times with PBS, placed into Tissue-Tek (Sakura Finetek, Torrance, CA, USA), and frozen at –80°C for 24 hours. Sections (8 μm) were fixed with 99% cold acetone for two minutes, washed three times with PBS, then blocked with skim milk with PBS for 30 minutes. The corneas were incubated with primary rat anti-F4/80 (1:500; Abd Serotec), podoplanin (1:500; Reliatech), or LYVE-1 (1:500) for 2 hours at room temperature, then washed, blocked, and secondary Cy3-conjugated donkey anti-rabbit (1:2500; Jackson ImmunoResearch) or FITC-conjugated goat anti-rat (1:2500; Jackson ImmunoResearch) were added for 30 minutes, followed by washing. The samples then were washed with PBS and mounted with VECTASHIELD and DAPI (Vector Laboratories, Inc., Burlingame, CA, USA). Sections were analyzed under a confocal microscope (LSM 710; Carl Zeiss Meditec).

Ear Wound Healing and Drainage Model

The mice were anesthetized with IP injections of ketamine (3 mg) and xylazine (0.01 mg). Full-thickness and excisional skin wounds (one per mouse) were created on the central portion of the ear using 2-mm skin biopsy punches. The mice were injected via tail vein with PMab-1 (100 μg) or PBS on postoperative days 0, 1, 2, 3, and 5. After 7 days of treatment with PMab-1, an intravital lymphatic permeability assay was conducted as described previously.[26] Indian ink (1 μL) was injected intradermally at the inner surface of the rim of the wound area with a 10-μL Hamilton syringe, to visualize the lymphatic vessels. The ear was photographed at 5 minutes after injection.

Evaluation of Ear Lymphatic Vessel-Like Structures

Seven days after the operation, the ear was excised, rinsed 3 times in PBS, mounted in Tissue-Tek, and frozen at –80°C. Cryosections of the ears were fixed in acetone for 1 minute and then rinsed 3 times in PBS, blocked with 3% skim milk, and incubated for 4 hours at 4°C with rabbit anti-mouse LYVE-1 and podoplanin. The tissues then were washed and stained with Cy3 or FITC-conjugated secondary antibody (1:2000; Jackson ImmunoResearch Laboratories). Skin thickness was measured on day 7. Lymphatic vessels were visualized on each postoperative day using LYVE-1 antibody, and the number of

Investigative Ophthalmology & Visual Science

LYVE-1–positive vessels were counted in a 400 × 200-μm section of the skin. Sections were analyzed under a fluorescence microscope (Olympus) in the same manner as the corneal model.

Collection and Culture of mps From the Peritoneal Cavity

Thioglycollate-induced mps were collected from the peritoneal cavity (PECs)[27] of healthy male C57BL/6 (8–10 weeks old) mice.[21] The PECs were washed, resuspended, and cultured (24 hours at 37°C in 5% CO_2; 10^6 cell/plate) in 35-mm culture plates in an RPMI 1640 medium containing 10% BSA (Sigma-Aldrich, St. Louis, MO, USA), 1×10^{-5} M 2-mercaptoethanol (Sigma-Aldrich), 10 mM HEPES, 0.1 mM nonessential amino acid, 1 mM sodium pyruvate, 100 U/mL penicillin, and 100 μg/mL streptomycin (Bio Whittaker, Walkersville, MD, USA). Adherent cells were harvested 24 hours later. To examine the effect of PMab-1 on inflammation, PECs were stimulated with either lipopolysaccharide (LPS; 1 μg/mL) or IFN-γ (200 ng/mL), or LPS (1 μg/mL) + IFN-γ (200 ng/mL), and cultured for 24 hours in the same media with the addition of 0, 1, 10, or 100 μg/mL PMab-1.

Western Blot Analysis and ELISA

Podoplanin, CLEC-2, NF-κB, and mitogen-activated protein kinase (MAPK) pathway (p38, p44/p42 [ERK], SAPK/JNK) expression was detected by a Western blot analysis using rabbit anti-mouse podoplanin, mouse monoclonal CLEC-2D antibody (Abcam, Cambridge, UK), rabbit anti-mouse NF-κB, rabbit anti-mouse p–NF-κB, rabbit anti-mouse p38/MAPK, rabbit anti-mouse p-p38/MAPK, rabbit anti-mouse p44/42/MAPK (ERK), rabbit anti-mouse p-p44/42/MAPK (p-ERK), rabbit anti-mouse SAPK/JNK, and rabbit anti-mouse p-SAPK/JNK (Cell Signaling Technology, Inc., Beverly, MA, USA). The TNF-α secretion was measured in supernatant collected from mps culture by ELISA; sample supernatants were used without dilution. Standard controls (1000, 500, 250, 125, 62.5, 31.3, and 15.6 pg/mL) and samples were incubated in 96-well plates. The capture and detection antibody pairs used were anti-mouse TNF (BD Biosciences, San Jose, CA, USA) and biotinylated anti-mouse TNF (BD Biosciences).

Tube Formation Assay

Tube formation assays were performed as described previously.[28] Human LECs were grown on fibronectin-coated 24-well plates until confluent. Next, 0.5 mL of neutralized isotonic bovine dermal collagen type I (Vitrogen; Celtrix Laboratories, Palo Alto, CA, USA) was added to the cells in the presence or absence of anti-human podoplanin antibody NZ-1 (Catalogue number, 11-009; 1, 10, 100 μg/mL; Angio Bio Co., Del Mar, CA, USA). After incubation at 37°C for 24 hours, the cells were fixed with 4% paraformaldehyde for 30 minutes at 4°C. Before lymphatic endothelial cells form tubes in collagen gels, endothelial cells connect with each other to form tubes in vitro. Representative images were captured, and the total length of the tube-like structures per area was measured using Image J software. All studies were performed in triplicate.

Statistical Analysis

Data were expressed as means ± SEM. Kaplan-Meier survival curves were used to compare graft survival. A Student's *t*-test was used to analyze the lymphangiogenesis inflammation response; $P < 0.05$ was considered significant.

Results

PMab-1 Suppressed Lymphatic Vessel Growth and mps Infiltration in the Corneal Suture-Placement Model

We investigated whether podoplanin inhibition could enhance lymphangiogenesis and mps infiltration under inflammatory conditions. We examined corneal lymphangiogenesis in mice corneas. There was less lymphangiogenesis in PMab-1–treated mouse corneas compared to those treated with PBS ($P < 0.05$). Moreover, there seemed to be less branching of lymphatic vessels compared to control (Figs. 1A, 1B). To investigate whether podoplanin is involved in inflammation, such as mps infiltration, we stained the sections with F4/80 to visualize mps in the corneal suture-placement model. F4/80 staining was detected around the LYVE-1^+ lymphatic vessels in the control group. A few mps were seen in the PMab-1–treated group (Figs. 1C, 1D).

Effect of PMab-1 on Lymphatic Vessel Growth, mps Infiltration and Graft Survival in a Corneal Transplantation Model

From previous experiments, we showed that PMab-1 reduced lymphangiogenesis, mps infiltration. It has been reported that lymphangiogenesis and inflammation are risk factors for transplantation rejection, and blocking them contributes to extending graft survival.[29–31] We used a corneal transplantation model to investigate whether the antilymphangiogenesis and anti-inflammatory effects of PMab-1 also can suppress graft rejection.

As expected, PMab-1 dramatically reduced mp infiltration (Figs. 2A, 2B). However, we were unable to find significant differences in lymphangiogenesis in the corneal transplantation model (Figs. 2A, 2B). PMab-1 administration extended graft survival in the corneal transplantation mice with a graft survival rate of 85% compared to 40 for control ($P = 0.0259$, Fig. 2C).

PMab-1 Suppressed Lymphangiogenesis in the Ear Wound-Healing Model

We next examined whether podoplanin is involved in wound healing–associated lymphatic vessel formation in another tissue, such as ear skin. The skin wound was created on the central portion of the ear to examine lymphangiogenesis during the wound-healing process. Lymphatic vessel growth in the PMab-1–treated mouse was less than in the PBS-treated mice ($P < 0.05$; Figs. 3D, 3E). This result revealed that lymphangiogenesis was significantly suppressed in PMab-1–treated mice compared to PBS-treated control mice. Moreover, lymphatic vessels in the wounded area in the PMab-1–treated group were larger than in the PBS-treated control group. Also, PMab-1 treatment suppressed lymphatic flow by downregulating lymphatic formation and enlarging the lymphatic vessels. (Fig. 3C). Thickness of the PMab-1–treated mouse ears were greater than in the PBS-treated control mice ($P < 0.05$; Figs. 3A, 3B).

Effect of PMab-1 on mps Activation Under Inflamed Condition

To determine whether podoplanin is involved in mp activation, we confirmed that podoplanin was expressed in mps and the lymphatic endothelium in histological sections. In particular, we found that in the ear wound healing model, the walls of the

Investigative Ophthalmology & Visual Science

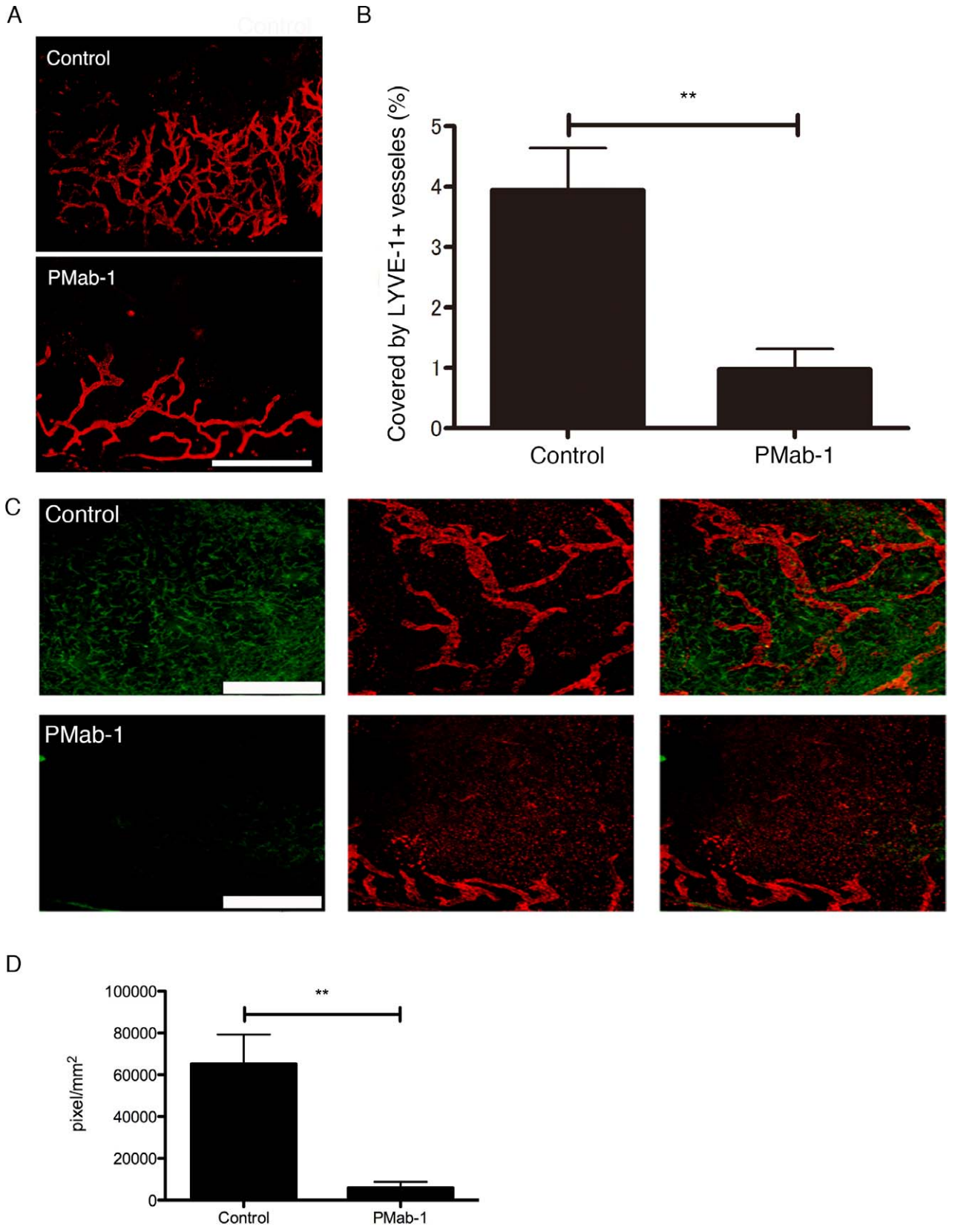

Figure 1. Effect of PMab-1 on lymphangiogenesis in the mouse corneal suture model. (**A**) Lymphangiogenesis (LYVE-1, *red*) in the PMab-1– or PBS-treated mouse cornea 7 days after suture placement. (**B**) Quantification of lymphangiogenesis in the corneal suture model assay ($n = 5$, each group). $^{**}P = 0.0095$. (**C**) The mps (F4/80, *green*), lymphangiogenesis (LYVE-1, *red*), and overlay in PBS- (*upper boxes*) and PMab-1– (*lower boxes*) treated mouse cornea 7 days after suture placement. *Scale bar* indicates 300 μm. (**D**) Quantification of the number of mps in the corneal suture model assay ($n = 5$, each group). $^{**}P = 0.0023$.

Investigative Ophthalmology & Visual Science

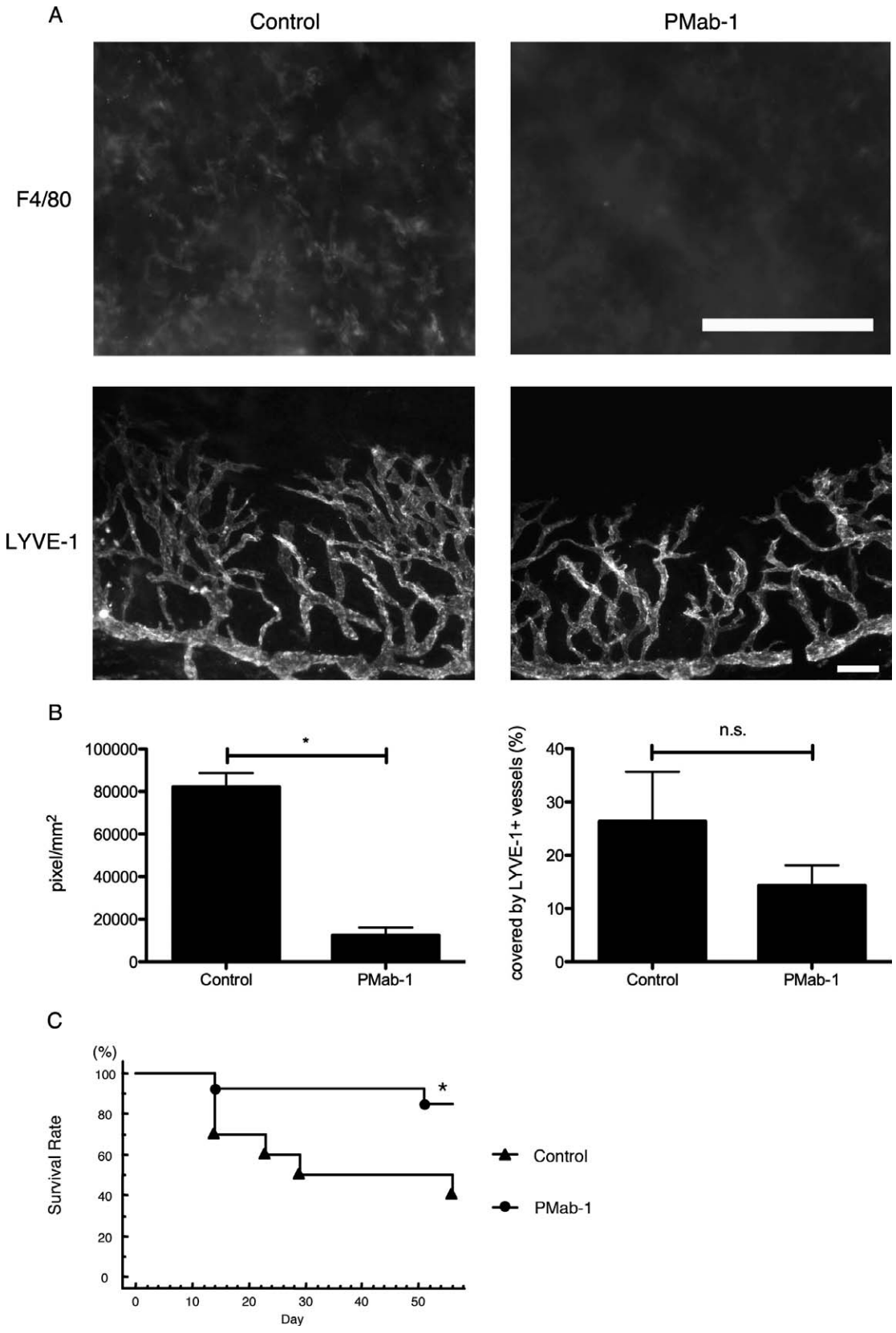

Figure 2. Effect of PMab-1 on graft survival in the corneal transplantation model. (**A**) Fluorescence micrograph indicating mps (F4/80) and lymphangiogenesis (LYVE-1) in the PMab-1– and PBS-treated mouse corneas 7 days after corneal transplantation. (**B**) Quantification of the number of mps (*$P = 0.0286$) and of lymphangiogenesis in the corneal transplantation model assay ($n = 5$, each group). n.s., no significant difference. (**C**) Survival rate in the corneal transplantation mice treated with PMab-1 ($n = 13$) or PBS for control ($n = 12$). *$P = 0.0259$.

Investigative Ophthalmology & Visual Science

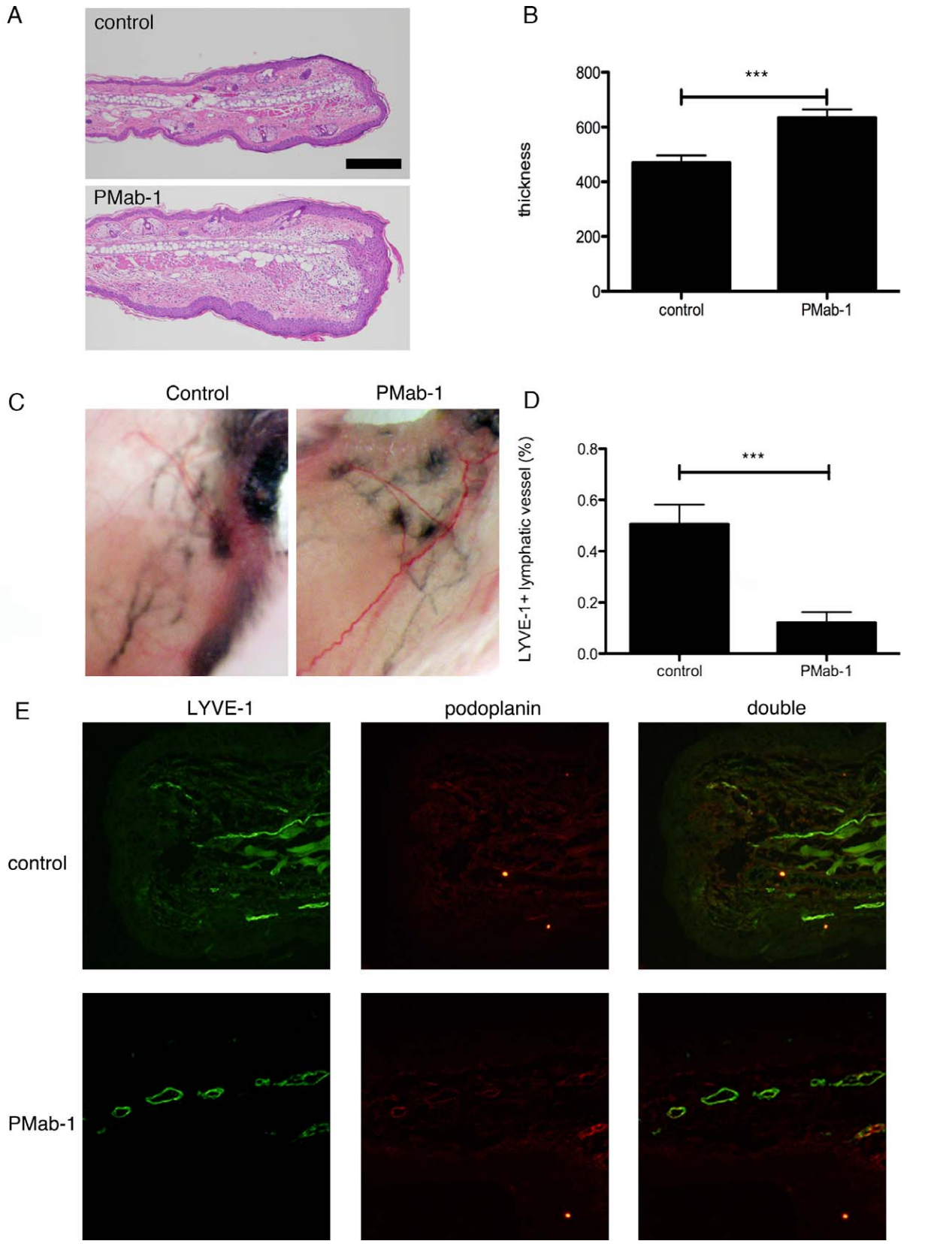

Figure 3. Lymphangiogenesis in the ear section model assay. (**A**) Photograph of hematoxylin and eosin-stained paraffin sections of PMab-1– or PBS-treated mouse ear 7 days after punch biopsies. *Scale bar*: 100 μm. (**B**) Quantification of thickness in the ear section model assay ($n = 5$, each group). $^{***}P = 0.0065$. (**C**) Indian ink injection in the ear wound healing model. The fluorescence micrograph indicated lymphatic morphology in the ear skin wound healing model. *Green*, LYVE-1; *red*, podoplanin. (**D**) Quantification of lymphangiogenesis in the ear section model assay ($n = 5$, each group). $^{***}P = 0.0040$. (**E**) Lymphangiogenesis (LYVE-1; *green*; podoplanin, *red*) in the PMab-1– or PBS-treated mouse ear 7 days after punch biopsies.

Investigative Ophthalmology & Visual Science

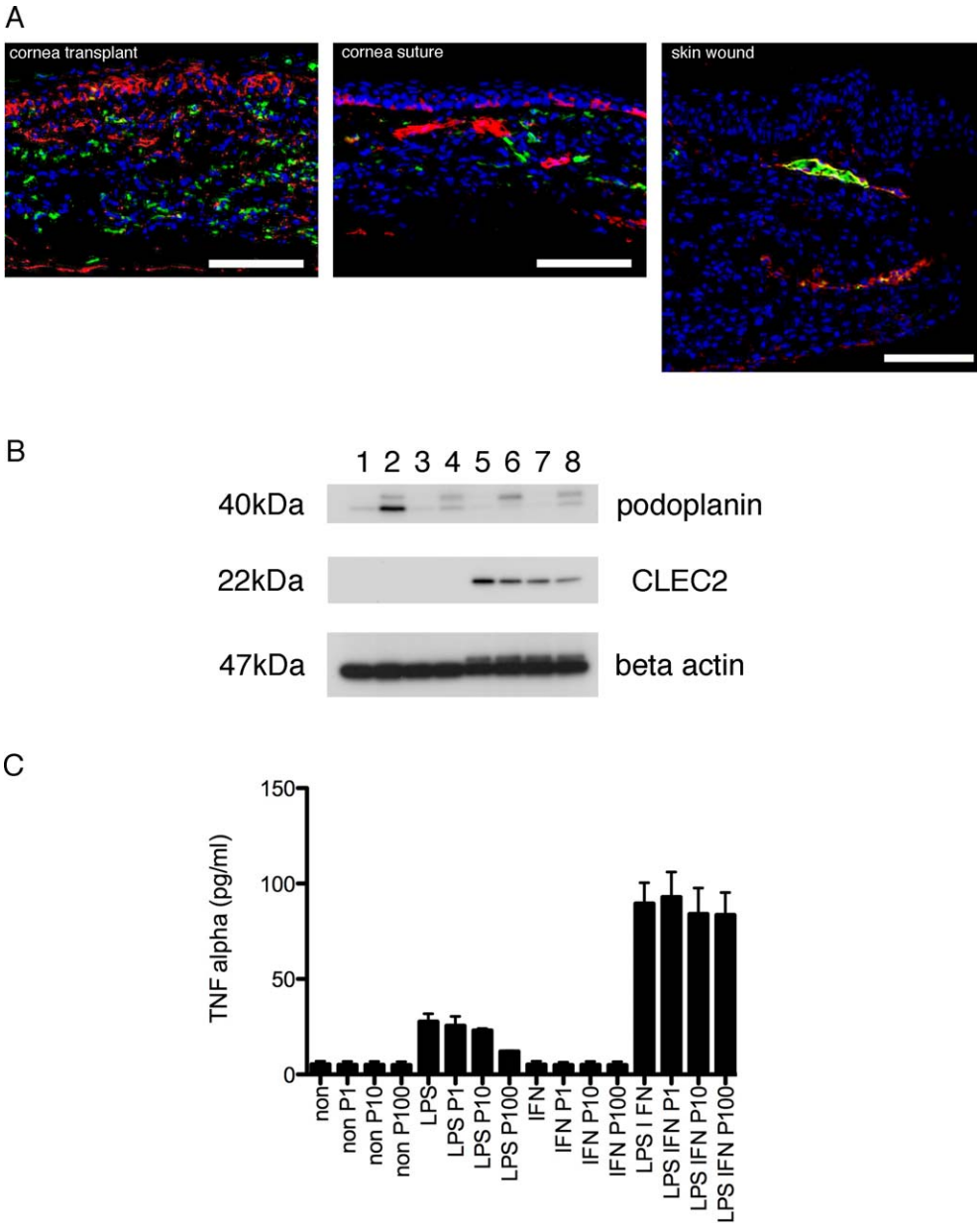

Figure 4. Podoplanin expression and TNF-α secretion from PECs. (**A**) Histological demonstration of podoplanin (*red*) and F4/80 (*green*) expression in the corneal transplantation, corneal suture placement and ear wound healing model. Cell nuclei were stained with DAPI (*blue*). *Scale bars*: 100 μm. (**B**) Western blot analysis of podoplanin and CLEC-2. β-Actin was used for control in the lower line. The PECs were stimulated with LPS (1 μg/mL) and IFN-γ (I, 200 ng/mL) as follows: Lane 1, non; Lane 2, LPS; Lane 3, IFN-γ; Lane 4, LPS+IFN-γ; Lane 5, non+PMab-1 (100 μg/mL); Lane 6, LPS+PMab-1 (100 μg/mL); Lane 7, IFN-γ+PMab-1 (100 μg/mL); Lane 8, LPS+IFN-γ+PMab-1 (100 μg/mL). (**C**) The TNF-α secretion from PECs stimulated with LPS or IFN-γ or LPS+IFN-γas measured by ELISA. The LPS dose was 1 μg/mL and IFN-γ dose was 200 ng/mL. P1, PMab-1, 1 μg/mL; P10, PMab-1, 10 μg/mL; and P100, PMab-1, 100 μg/mL.

lymphatic vessel-like structures expressed both F4/80 and podoplanin (Fig. 4A). Moreover, we used ELISA to examine proinflammatory cytokines from mps after stimulation with LPS or IFN-γ-or, LPS+IFN-γ. To compare the expression pattern of podoplanin and CLEC-2 in mps with different stimulation, we performed Western blot analysis. Podoplanin expression increased with LPS stimulation, but not with IFN-γ or LPS+IFN-γ stimulation. (Fig. 4B). The TNF-α secretion was higher when the PECs were stimulated with LPS+IFN-γ compared to LPS alone, but TNF-α secretion did not increase when the PECs were stimulated with IFN-γ alone (Fig. 4C). The TNF-α secretion from PECs after LPS stimulation was significantly reduced by PMab-1 treatment ($P < 0.03$, Fig. 4C) in a concentration-dependent manner. However, PMab-1 treatment did not alter TNF-α secretion after LPS+IFN-γ stimulation (Fig. 4C). The CLEC-2 expression increased with PMab-1 treatment to block podoplanin (Fig. 4B).

The Effect of PMab-1 on the PEC Inflammation Pathway

As noted in the previous section, inflammation with LPS stimulation increased podoplanin expression, and that TNF-α secretion induced by stimulation with LPS alone, but not with LPS and INF-γ, was suppressed by PMab-1. Therefore, we

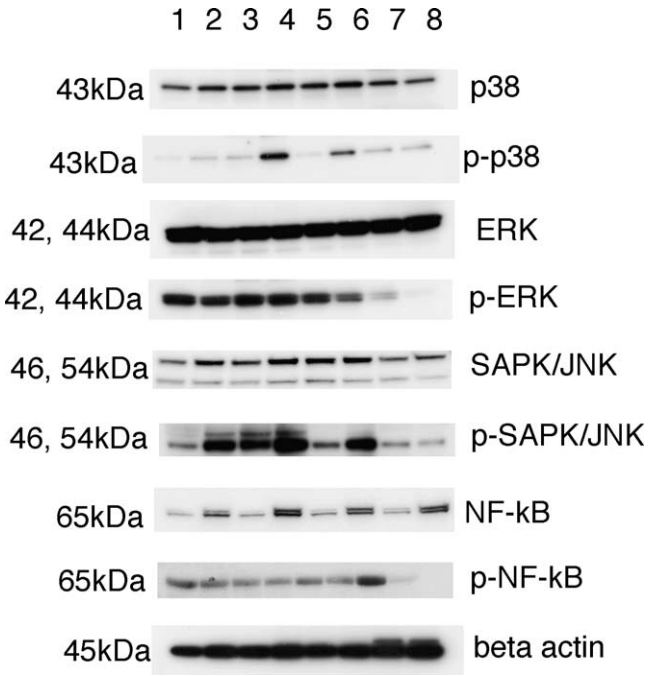

Figure 5. Effect of PMab-1 on PEC inflammation. Western blot analysis of NF-κB, p–NF-κB, and the MAPK pathways: p38, p-p38, p44/42 (ERK), p-p44/42 (p-ERK), andSAPK/JNK, p-SAPK/JNK . β-Actin was used for control in the lower line. The PECs were stimulated with LPS (1 μg/mL), and PMab-1 as follows: Lane 1, non; Lane 2, LPS; Lane 3, non+PMab-1 (1 μg/mL); Lane 4, LPS+PMab-1 (1 μg/mL); Lane 5, non+PMab-1 (10 μg/mL); Lane 6, LPS+PMab-1 (10 μg/mL); Lane 7, non+PMab-1 (100 μg/mL); Lane 8, LPS+PMab-1 (100 μg/mL).

investigated which inflammation pathways were activated and which were blocked using PMab-1.

First, we examined podoplanin expression change in PECs after treatment with PMab-1. Podoplanin expression on PECs was increased when stimulated with LPS (Fig. 4B). PMab-1 reduced podoplanin expression on PECs in a concentration-dependent manner.

Inflammation-related pathways, such as NF-κB and MAPK, were examined by Western blot analysis to determine which were involved in podoplanin expression. The PMab-1 affected activation of the NF-κB pathway, the SPK/JNK, p44/p42 (ERK), and p38 (MAPK pathways) were decreased when treated with PMab-1 (Fig. 5). Therefore, our data showed that the LPS-induced inflammatory pathway, such as MAPK and NF-κB pathways, were affected by PMab-1.

Effect of Anti-Human Podoplanin Antibody on Human LEC Tube Formation

To investigate the involvement of podoplanin in lymphatic vessel formation in vitro, we used the anti-human podoplanin antibody NZ-1 and determined its effect on tube formation in human LECs. Hirakawa et al.[32] reported that 24 hours after seeding onto Matrigel-coated culture tissues, LECs efficiently formed network-like structures in vitro. Kajiya et al.[33] reported that hepatocyte growth factor stimulation promoted the in vitro formation of lymphatic tubes using this method. In this study, we used the same method and confirmed that LECs formed tube-like structures in the control group, as described previously (Fig. 6A). Tube formation was significantly suppressed by anti-human podoplanin antibody in a concentration-dependent manner (Fig. 6B).

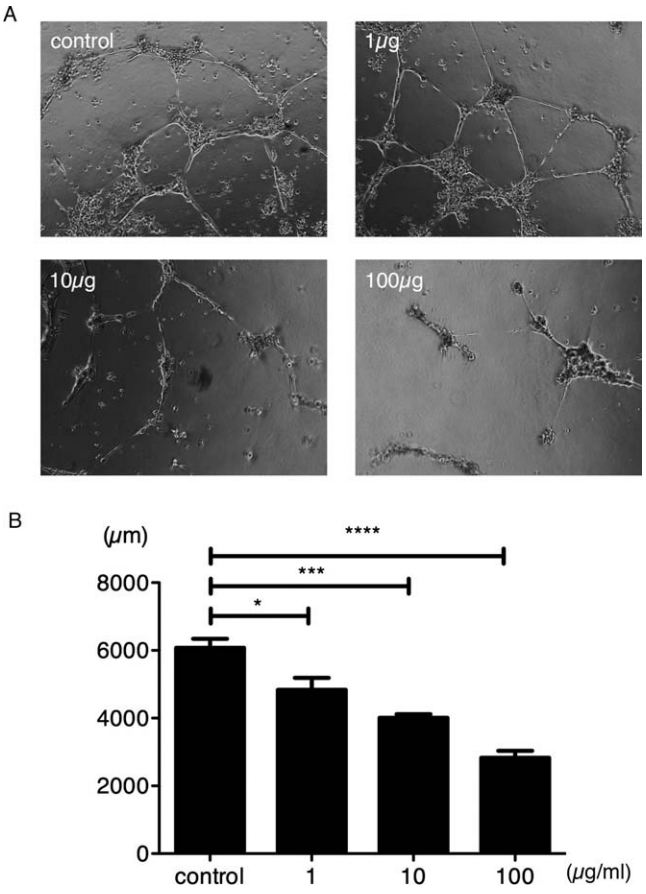

Figure 6. Effect of anti-human podoplanin antibody on hLECs. (**A**) Photograph of a representative tube formation assay with a control mouse and IgG or NZ-1 (1, 10, or 100 μg/mL) treatment. (**B**) Quantification of tube formation with NZ-1 ($n = 4$, each group). $^{*}P = 0.0139$ (control versus NZ-1 [1 μg/mL]), $^{*}P = 0.0114$ (control versus NZ-1 10 μg/mL), $^{****}P < 0.0001$ (control versus NZ-1 100 μg/mL).

Discussion

In this study, we demonstrated that the anti-mouse podoplanin antibody PMab-1 could dramatically suppress lymphangiogenesis and mps infiltration in the mouse corneal suture model. The PMab-1 antibody also suppressed mps infiltration and graft rejection after corneal transplantation. In another in vivo experiment, the ear wound-healing model, lymphatic vessel density, and lymphatic flow were less in the PMab-1 treatment group compared to control. As a result, in the PMab-1 treatment group, the tissue might remain thick during the healing process due to reduced lymphatic drainage. Moreover, anti-podoplanin treatment reduced mp-induced inflammation, and, more surprisingly, it directly inhibited lymphatic vessel formation in a dose-dependent manner in an in vitro assay using human LECs.

It has been shown that podoplanin has a critical role in separating lymphatic vessel endothelial cells from the cardinal vein when the vascular network is developing in the embryonic stage.[16,17] However, the role of podoplanin in lymphangiogenesis under inflammatory conditions in adulthood, such wound healing, still is not well investigated. In the corneal suture model, our data showed that lymphangiogenesis was dramatically suppressed by PMab-1. Previously, it was reported that lymphangiogenesis was conducted by mps density in tissue and the secretion of cytokines from local tissue or mps. Our previous data showed that mps that had

Investigative Ophthalmology & Visual Science

accumulated around lymphatic vessels had a critical role in their maintenance.[22] To our knowledge, we were the first to suggest that mps deletion could induce lymphatic regression.[22] In the present study, the number of mps around LYVE-1+ lymphatic vessels was greater in the corneas of the control group than the PMab-1–treated group; only a few mps could be seen in the PMab-1–treated group. Moreover, in the ear wound model, podoplanin-expressing lymphatic-like structures also expressed F4/80. This phenomenon was a similar occurrence as our previous report.[34] Thus, it was hypothesized that podoplanin had a critical role for mps infiltration.

It has been reported that lymphangiogenesis and inflammation are risk factors for transplantation rejection, and that blocking them contributes to graft survival. Yamagami et al.[35] reported that dissection of regional lymph nodes from the host mouse in the transplantation model could completely suppress the rejection reaction. Moreover, Cursiefen et al.[36] reported that suppressing lymphangiogenesis could suppress the rejection reaction. Therefore, suppressing the afferent phase of the rejection reaction, such as the antigen presentation process, might inhibit the rejection reaction in the corneal transplantation model. Our previous results also showed that manipulating the thiol redox status in mps could suppress mps-induced lymphangiogenesis and rejection reaction in the corneal transplantation model. In the present study, we used the corneal transplantation model to investigate whether the PMab-1 antilymphangiogenesis and anti-inflammatory reactions also suppress the rejection reaction. The PMab-1 antibody administration significantly suppressed the rejection reaction in the mouse corneal transplantation model as expected.

Previously, it was reported that podoplanin on myeloid cells was associated with inflammatory responses, and also that LPS-stimulated dendritic cells (DCs) cultured on spleen stromal cells that express podoplanin increased amounts of cytokines.[19] To confirm this, we investigated the role of podoplanin in inflammatory reactions in mps using PMab-1. It has been shown that podoplanin expression is markedly upregulated on bone marrow-derived mps following LPS stimulation.[20] Our results agreed with this study and used Western blot to detect podoplanin expression. Interestingly, podoplanin expression on mps was much higher after LPS stimulation alone compared to IFN-γ stimulation alone and LPS+IFN-γ stimulation. Podoplanin expression on mps might be influenced by LPS stimulation via the toll-like receptor (TLR) 4 pathway,[37] but not by the IFN-stimulating pathway.

The TNF-α was higher in mps treated with LPS+IFN-γ compared to LPS alone. In the present study, PMab-1 decreased the levels of TNF-α induced by LPS stimulation alone, but not LPS+IFN-γ stimulation. The ability of PMab-1 to block LPS-induced inflammatory reactions and also podoplanin may be associated mainly with the inflammation pathway induced by LPS. We examined several inflammatory pathways by Western blot to investigate which pathway was associated with podoplanin. The protein level of NF-κB signal tended to be higher in mps after LPS+IFN-γ stimulation versus LPS alone. In contrast, SPK/JNK, p44/p42 (ERK), and p38 (MAPK pathways) tended to be higher after LPS stimulation alone compared to LPS+IFN-γ stimulation. Intriguingly, our present result indicated that p44/42 (ERK), JNK/SAPK, and p38 are related to the MAPK inflammatory pathways as they were suppressed by PMab-1 (Fig. 5). Moreover, PMab-1 also suppressed the NF-κB signal. Our investigation indicates that podoplanin is mainly involved in the LPS stimulation pathway, such as MAPK and NF-κB inflammatory pathways. Further investigation is needed to provide more detail about this mechanism.

We showed that anti-mouse podoplanin antibody PMab-1 suppressed lymphangiogenesis in the corneal suture and ear wound-healing model in vivo due to suppression of mps function. Previously, it was reported that podoplanin deletion caused malformation of lymphatic vessel in embryos due to interference between platelet and podoplanin interactions on vascular endothelial cells. In the present study, we showed that an anti-human podoplanin antibody (NZ-1) had a direct effect on podoplanin in human LECs. Our results indicated that NZ-1 dramatically suppressed tube formation in human LECs, and suggested that podoplanin had a direct effect on mps, as well as the lymphatic endothelium. However, our in vivo experiments did not have any direct evidence that podoplanin affects lymphatic endothelium. Our present experiment suggested that PMab-1 affected drainage function in the ear skin wound healing model. Drainage function appeared to be reduced compared to the controls with PMab-1 treatment. Based on our data, we speculated that lymphatic vessel formation may decrease, and the lymphatic vessels in the wound area may become enlarged, which would affect drainage. Further investigation is needed to provide more detail about the mechanism underlying this phenomenon.

The findings of this study showed that blocking podoplanin inhibits lymphatic growth associated with corneal and ear wound healing in mice, and mps inflammation. These data suggested that podoplanin is a novel therapeutic target for lymphangiogenesis and mps-related inflammation.

Acknowledgments

The authors thank Wendy Chao and Tim Hilts for editing and critical reading of this manuscript.

Supported by Research Grant KAKEN 23592613; and in part by the Platform for Drug Discovery, Informatics, and Structural Life Science; and by Regional Innovation Strategy Support Program from the Ministry of Education, Culture, Sports, Science, and Technology of Japan. The authors alone are responsible for the content and writing of the paper.

Disclosure: **Y. Maruyama**, None; **K. Maruyama**, None; **Y. Kato**, None; **K. Kajiya**, None; **S. Moritoh**, None; **K. Yamamoto**, None; **Y. Matsumoto**, None; **M. Sawane**, None; **D. Kerjaschki**, None; **T. Nakazawa**, None; **S. Kinoshita**, None

References

1. Breiteneder-Geleff S, Soleiman A, Kowalski H, et al. Angiosarcomas express mixed endothelial phenotypes of blood and lymphatic capillaries: podoplanin as a specific marker for lymphatic endothelium. *Am J Pathol*. 1999;154:385–394.
2. Yuan P, Temam S, El-Naggar A, et al. Overexpression of podoplanin in oral cancer and its association with poor clinical outcome. *Cancer*. 2006;107:563–569.
3. Tong L, Yuan S, Feng F, Zhang H. Role of podoplanin expression in esophageal squamous cell carcinoma: a retrospective study. *Dis Esophagus*. 2012;25:72–80.
4. Mishima K, Kato Y, Kaneko MK, Nishikawa R, Hirose T, Matsutani M. Increased expression of podoplanin in malignant astrocytic tumors as a novel molecular marker of malignant progression. *Acta Neuropathol*. 2006;111:483–488.
5. Martin-Villar E, Scholl FG, Gamallo C, et al. Characterization of human PA2.26 antigen (T1alpha-2, podoplanin), a small membrane mucin induced in oral squamous cell carcinomas. *Int J Cancer*. 2005;113:899–910.
6. Kato Y, Kaneko M, Sata M, Fujita N, Tsuruo T, Osawa M. Enhanced expression of Aggrus (T1alpha/podoplanin), a platelet-aggregation-inducing factor in lung squamous cell carcinoma. *Tumour Biol*. 2005;26:195–200.
7. Dumoff KL, Chu C, Xu X, Pasha T, Zhang PJ, Acs G. Low D2-40 immunoreactivity correlates with lymphatic invasion and nodal metastasis in early-stage squamous cell carcinoma of the uterine cervix. *Mod Pathol*. 2005;18:97–104.

8. Kato Y, Kaneko MK, Kuno A, et al. Inhibition of tumor cell-induced platelet aggregation using a novel anti-podoplanin antibody reacting with its platelet-aggregation-stimulating domain. *Biochem Biophys Res Commun*. 2006;349:1301–1307.
9. Kawase A, Ishii G, Nagai K, et al. Podoplanin expression by cancer associated fibroblasts predicts poor prognosis of lung adenocarcinoma. *Int J Cancer*. 2008;123:1053–1059.
10. Kunita A, Kashima TG, Morishita Y, et al. The platelet aggregation-inducing factor aggrus/podoplanin promotes pulmonary metastasis. *Am J Pathol*. 2007;170:1337–1347.
11. Renyi-Vamos F, Tovari J, Fillinger J, et al. Lymphangiogenesis correlates with lymph node metastasis, prognosis, and angiogenic phenotype in human non-small cell lung cancer. *Clin Cancer Res*. 2005;11:7344–7353.
12. Nakazawa Y, Takagi S, Sato S, et al. Prevention of hematogenous metastasis by neutralizing mice and its chimeric anti-Aggrus/podoplanin antibodies. *Cancer Sci*. 2011;102:2051–2057.
13. Kato Y, Vaidyanathan G, Kaneko MK, et al. Evaluation of anti-podoplanin rat monoclonal antibody NZ-1 for targeting malignant gliomas. *Nucl Med Biol*. 2010;37:785–794.
14. Kaneko MK, Kunita A, Abe S, et al. Chimeric anti-podoplanin antibody suppresses tumor metastasis through neutralization and antibody-dependent cellular cytotoxicity. *Cancer Sci*. 2012;103:1913–1919.
15. Chandramohan V, Bao XH, Kaneko MK, et al. Recombinant anti-podoplanin (NZ-1) immunotoxin for the treatment of malignant brain tumors. *Int J Cancer*. 2013;132:2339–2348.
16. Bertozzi CC, Hess PR, Kahn ML. Platelets: covert regulators of lymphatic development. *Arterioscler Thromb Vasc Biol*. 2010;30:2368–2371.
17. Uhrin P, Zaujec J, Breuss JM, et al. Novel function for blood platelets and podoplanin in developmental separation of blood and lymphatic circulation. *Blood*. 2010;115:3997–4005.
18. Schacht V, Ramirez MI, Hong YK, et al. T1alpha/podoplanin deficiency disrupts normal lymphatic vasculature formation and causes lymphedema. *EMBO J*. 2003;22:3546–3556.
19. Mourao-Sa D, Robinson MJ, Zelenay S, et al. CLEC-2 signaling via Syk in myeloid cells can regulate inflammatory responses. *Eur J Immunol*. 2011;41:3040–3053.
20. Kerrigan AM, Navarro-Nunez L, Pyz E, et al. Podoplanin-expressing inflammatory macrophages activate murine platelets via CLEC-2. *J Thromb Haemost*. 2011;10:484–486.
21. Maruyama K, Ii M, Cursiefen C, et al. Inflammation-induced lymphangiogenesis in the cornea arises from CD11b-positive macrophages. *J Clin Invest*. 2005;115:2363–2372.
22. Maruyama K, Nakazawa T, Cursiefen C, et al. The maintenance of lymphatic vessels in the cornea is dependent on the presence of macrophages. *Invest Ophthalmol Vis Sci*. 2012;53:3145–3153.
23. Cursiefen C, Chen L, Borges LP, et al. VEGF-A stimulates lymphangiogenesis and hemangiogenesis in inflammatory neovascularization via macrophage recruitment. *J Clin Invest*. 2004;113:1040–1050.
24. Nakao S, Kuwano T, Tsutsumi-Miyahara C, et al. Infiltration of COX-2-expressing macrophages is a prerequisite for IL-1 beta-induced neovascularization and tumor growth. *J Clin Invest*. 2005;115:2979–2991.
25. Kaji C, Tsujimoto Y, Kato Kaneko M, Kato Y, Sawa Y. immunohistochemical examination of novel rat monoclonal antibodies against mouse and human podoplanin. *Acta Histochem Cytochem*. 2012;45:227–237.
26. Kajiya K, Hirakawa S, Detmar M. Vascular endothelial growth factor-A mediates ultraviolet B-induced impairment of lymphatic vessel function. *Am J Pathol*. 2006;169:1496–1503.
27. Kezuka T, Streilein JW. In vitro generation of regulatory CD8+ T cells similar to those found in mice with anterior chamber-associated immune deviation. *Invest Ophthalmol Vis Sci*. 2000;41:1803–1811.
28. Sawane M, Kidoya H, Muramatsu F, Takakura N, Kajiya K. Apelin attenuates UVB-induced edema and inflammation by promoting vessel function. *Am J Pathol*. 2011;179:2691–2697.
29. Zheng Y, Lin H, Ling S. Clinicopathological correlation analysis of (lymph) angiogenesis and corneal graft rejection. *Mol Vis*. 2011;17:1694–1700.
30. Cursiefen C, Chen L, Dana MR, Streilein JW. Corneal lymphangiogenesis: evidence, mechanisms, and implications for corneal transplant immunology. *Cornea*. 2003;22:273–281.
31. Cursiefen C, Cao J, Chen L, et al. Inhibition of hemangiogenesis and lymphangiogenesis after normal-risk corneal transplantation by neutralizing VEGF promotes graft survival. *Invest Ophthalmol Vis Sci*. 2004;45:2666–2673.
32. Hirakawa S, Hong YK, Harvey N, et al. Identification of vascular lineage-specific genes by transcriptional profiling of isolated blood vascular and lymphatic endothelial cells. *Am J Pathol*. 2003;162:575–586.
33. Kajiya K, Hirakawa S, Ma B, Drinnenberg I, Detmar M. Hepatocyte growth factor promotes lymphatic vessel formation and function. *EMBO J*. 2005;24:2885–2895.
34. Maruyama K, Asai J, Ii M, Thorne T, Losordo DW, D'Amore PA. Decreased macrophage number and activation lead to reduced lymphatic vessel formation and contribute to impaired diabetic wound healing. *Am J Pathol*. 2007;170:1178–1191.
35. Yamagami S, Dana MR. The critical role of lymph nodes in corneal alloimmunization and graft rejection. *Invest Ophthalmol Vis Sci*. 2001;42:1293–1298.
36. Cursiefen C, Cao J, Chen L, et al. Inhibition of hemangiogenesis and lymphangiogenesis after normal-risk corneal transplantation by neutralizing VEGF promotes graft survival. *Invest Ophthalmol Vis Sci*. 2004;45:2666–2673.
37. Schorey JS, Cooper AM. Macrophage signalling upon mycobacterial infection: the MAP kinases lead the way. *Cell Microbiol*. 2003;5:133–142.

Investigative Ophthalmology & Visual Science